The VLBI SOuthern Astrometry Project (SOAP)

Science team members (in alphabetic order)

Johannes Boehm
Alet de Witt
Sergei Gulyaev
Shinji Horiuchi
Jamie McCallum
Lucia McCallum
Tim Natusch
Leonid Petrov
Jonathan Quick
Fengchun Shu
Stuart Weston

The document is prepared by Leonid Petrov (email: Leonid.Petrov@lpetrov.net)

Version 1.0 of 2017.09.04

1 Summary

A program of VLBI southern hemisphere astrometry is proposed. The program utilizes available VLBI resources in the southern hemisphere. The final goal of the the VLBI SOuthern Astrometry Project (SOAP) program is to improve positions of all known VLBI sources at declinations $< -30^\circ$ **by a factor of five** to the level of 0.3 mas, derive their images, and determine jet directions.

2 The broad context

It is not an exaggeration to say that date September 15, 2016 split absolute astrometry into two epochs: before and after *Gaia*. It will take time to realize the magnitude of the change. A preliminary data release one (DR1) (Lindegren et al. 2016) presented results of a coarse solution with many corners cut and should be considered rather a preview of the *Gaia* catalogue. But it has demonstrated clearly that goals of *Gaia* will be fulfilled. The consequences of the data release are the following:

- Ground optical astrometry of objects stronger magnitude 21 in G filter is almost obliterated. Remaining areas where ground observations can be competitive are:
  - densification of the optical catalogue deeper than the *Gaia* cutoff around 21 mag;
  - densification of the catalogue towards weak red or infra-red sources not visible by *Gaia*;
  - monitoring asteroid orbits.

Table 1: Completeness of the RFC at 8 GHz derived by extrapolation of log N/ log S curve.

10 mJy	10%
30 mJy	31%
50 mJy	49%
80 mJy	69%
100 mJy	80%
120 mJy	87%
140 mJy	93%
150 mJy	95%
160 mJy	97%
170 mJy	99%

- It was found that roughly 50% VLBI sources have a counterpart with *Gaia*. As a detailed analysis of Petrov & Kovalev (2017a,b), Kovalev et al. (2017) showed, the differences VLBI and optical AGN positions exhibit a strong systematic pattern: *Gaia*/VLBI offsets are aligned along jet directions. Kovalev et al. (2017) interpret it as a manifestation of the presence of optical structure. The consequences of that discovery are
  - VLBI and *Gaia* AGNS positions will not be reconciled beyond 1–2 mas level. Further improvement of VLBI and/or *Gaia* accuracy will improve the accuracy of determination of these offsets, but will not eliminate them. That means we cannot transfer accurate *Gaia* optical position of an AGN and predict its VLBI position beyond 1–2 mas level.
  - Jitter in *Gaia* AGN positions at milliarcsecond level caused by source variability is predicted.
  - Analysis of the jitter in *Gaia* AGN positions and optical light curves opens a new window in observations of AGNs: in a case of strong variability it allows to localize the region of flares and the decompose the light curve into the contribution from the accretion disk, jet base (core), and extended jet.

From the other hand, completion of the astrometric analysis of VLBI Calibrator Surveys (VCS) 7,8, and 9 in 2017 ushers a gradual end of the extensive phase of VLBI absolute astrometry focused on the growth of the number of VLBI sources observed in the absolute astrometry source. By August 2017, the accumulative catalogue of absolute source positions reached 14, 768. The main goal of that extension was to provide a dense grid of calibrators than can be used as phase calibrators for imaging weak sources and for differential astrometry. Further growth will require significantly more efforts since effectiveness of surveys drops because the pool of calibrators with the high probability of being compact depletes. Considering the effectiveness of a search of the sources with correlated flux density > 50 mJy at a level of 20–30%, in order to double the number of sources in the RFC and reach the completeness at 50 mJy, we will need to observe over 50,000 candidate objects. This does not seem the optimal allocation of resources.

The growth of the number of calibrator sources was achieved by expense of accuracy. Accuracy 2–5 mas was sufficient for phase referencing applications. Table 2 shows the distribution of formal errors. VLBI position accuracy above the 0.1–0.3 mas (0.5–1.5 nrad) level is determined by the thermal noise. The systematic errors dominate below that level. Positions of only 20% sources are known to that level. Improvement in accuracy to the 0.1–0.3 mas level can

Table 2: Cumulative distribution of the RFC catalogue formal errors for 14,768 sources. Units: mas.

10%	0.2
20%	0.3
50%	0.9
80%	2.5
90%	5.2
95%	10.6

be achieved just by more astrometric observations of the target sources which positions are not known accurately.

The facts summarized above constrain the direction of future VLBI absolute astrometric programs:

- programs focused on a search of new calibrators will be limited to special areas of interest, such as the ecliptic plane or Galactic plane, or in the vicinity of the sources with probably counterparts, such as *Fermi*-detected γ-ray sources. Surveys of these style will be gradually fade out.

- Observing programs focused of improvement of source positions down to 0.3 mas level will become more common. The number of sources which positions can be improved, over 11,000 objects, requires a prioritization.

- Problems that require high accuracy (better than 3–10 mas):

  - space navigation. Position accuracy 1 nrad (0.2 mas) is required.

  - Determination of the so-called $\mathcal{O}_\mathrm{j}$ observable — the projection of the *Gaia*/VLBI offset onto the radio jet direction. Scientific analysis of $\mathcal{O}_\mathrm{j}$ requires position accuracy 0.3 mas and availability of high fidelity images that allow determination of jet direction with accuracy better 10°.

  - Determination of absolute positions of pulsars that have precise timing position. Accuracy 0.25–1.0 nrad of calibrator sources is required. The core-shifts of calibrator sources should be determined with the same accuracy.

  - Position of the sources used for space geodesy. Accuracy 1.0 nrad is needed. This problem is solved.

- Extension of the astrometric catalogue to low frequencies (below 1.7 GHz) by using the in-beam differential astrometry technique. Accuracy of these source positions derived from these observations is 2–5 mas and it is limited by the residual ionospheric contribution and the core-shift.

- Programs focused on observations of known RFC sources at higher frequencies (22 GHz and higher) for their imaging, evaluation of their flux density and determination of their suitability as calibrators at high frequencies.

- Suggested prioritization:

  - zone of special interest: a) ecliptic plane; b) Galactic plane; c) fields of multifrequency deep observations;

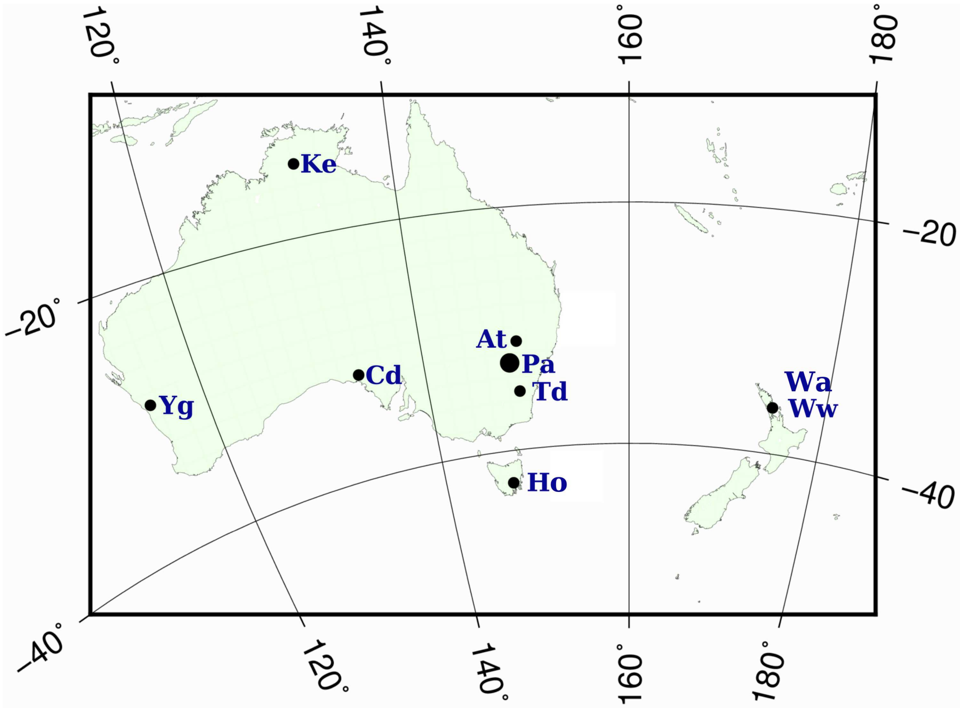

Figure 1: The southern VLBI network. Stations Hh or Ht (HARTRAO), 60 km north-west of Johannesburg, South Africa; stations Sh or T6 near Shanghai, and station Km at Kunming, south-east China, are not shown.

– sources with *Gaia* matches with bright counterparts;

– calibrators used for VLBI pulsar differential astrometry.

3 State of the VLBI absolute astrometry in the southern hemisphere

Before 2008, a strong disparity in the source distribution of the accumulative VLBI astrometric catalogue between southern and northern hemispheres was evident. In 2008–2016 1742 sources were observed with the Long Baseline Array Survey (LCS) program Petrov et al. (2011). Of them, 1336 were detected. Among 1336 detected sources, 1280 are with declinations $< -30°$ and 1170 at declinations $< -40°$. This program has eliminated the hemisphere disparity in source distribution down to 150 mJy and mitigated remaining disparity at low flux density levels. However, the stations of the LBA network lack dual-band receivers. Source positions derived using single-band 8.4 GHz group delays suffered from systematic errors caused by the mismodeled ionosphere at a level of 0.5–2.5 mas depending on the state of ionosphere. Besides, the observation mode, 1–3 scans per source on a network of 1700 km long did not result in high precision astrometry: even formal errors of 1/3 targets were worse than 2 mas.

At the moment, among the sources with declinations $< -40°$, positions of only 10% are known with accuracy better 0.3 mas. Positions of remaining 1049 sources can be improved with a dedicated astrometric program. The final goal of the the VLBI SOuthern Astrometry Project (SOAP) program is to improve positions of all known VLBI sources at declinations $< -30°$ to the level of 0.3 mas. The feasibility of the SOuthern Astrometric Program is determined by the availability of resources. At the moment, there are 6 sites at the southern hemisphere with

Table 3: The southern VLBI network. The LBA stations network. The typical System Equivalent Flux Density (SEFD) at 8.3 GHz at elevation angles > 45° is shown in the last column.

Code	Name	φ_{gc}	λ	Diam	SEFD
At	ATCA	-30°.15	149°.57	5 × 22 m	140 Jy
Ha	HARTRAO	-25°.74	27°.69	26 m	1200 Jy
Ht	HART15M	-25°.74	27°.69	15 m	1400 Jy
Ho	HOBART26	-42°.62	147°.44	26 m	850 Jy
Ke	KATH12M	-14°.28	132°.15	12 m	3500 Jy
Pa	PARKES	-32°.82	148°.26	64 m	50 Jy
Td	TIDBINBILLA	-35°.22	148°.98	34 m	120 Jy
Yg	YARRA12M	-28°.88	115°.35	12 m	3000 Jy
Wa	WARK30M	-36°.25	174°.66	30 m	900 Jy
Ww	WARK12M	-36°.25	174°.66	12 m	3000 Jy
Sh	SESHAN25	+30°.93	121°.20	25 m	600 Jy
T6	TIANMA65	+30°.93	121°.20	65 m	60 Jy
Km	KUNMING	+24°.88	102°.80	40 m	480 Jy

Table 4: Baseline sensitivity at Auscope antennas (Au means any of Ke, Yg, Hb, Ww) at X-band assuming 4 minute integration and 640 Mbps

baseline	SEFD	Flux 1σ	Flux det	flux SNR=15
	Jy	mJy	mJy	mJy
Au/Au	3500	19	115	285
Au/Ho Au/Hh Au/Wa	1800	9	60	135
Au/Td Au/Pa	650	3.5	21	52
Au/T6	450	2.4	15	36

S/X receivers: Ke, Yg, Ww with SEFD around 3500 Jy, Hh, Ho with SEFD around 1000 Jy and Td with SEFD 120 Jy. Td may observe mainly in short sessions of 4–8 hours long. Pa with SEFD 50 Jy is a part of ATNF astrometry program v561a and is not considered in this section. Wa with SEFD 900 Jy can observe in X-band only. Stations T6 ($\varphi = +30.9°$, SEFD 60 Jy) and Km ($\varphi = +24.9°$, SEFD 480 mJy) may observe sources in the declination band $[-30°, -45°]$. Table 4 shows the baseline sensitivity of the southern VLBI network assuming the experiments are conducted at 1024 Mbps and 10/16 bandwidth is allocated for the X-band and 6/16 bandwidth is allocated for the S-band. We do not know S-band flux densities for the majority of the sources at declinations below $-45°$. If a spectral index of a source is 0 (flat), and assuming sensitivity at S-band is the same as at X-band, the SNR will be a factor of $\sqrt{10/6} \approx 1.3$ times less. For the sources with spectral index $\ln(\sqrt{10/6})/\ln(2.2/8.6) = -0.2$, the SNR will be the same, and the SNR at S-band will be greater than at X-band for sources with spectral index < -0.2 (steeper).

Assuming 5 minute integration time and 160 MHz recorded bandwidth at X-band, 2bit per sample, table 4 demonstrates that for sources brighter 250 mJy the target SNR=15 will achieve at all 10 baselines of a 5-station network Ke-Yg-Ww-Hh-Ho. Sources with flux density in a range of [120, 250] mJy will still be detected at all 10 baselines, but the target SNR will be reached only at 6 baselines with Ho and Hh. Including Td or T6 will help to achieve SNR=15 at 5 baselines for sources with flux density in a range of [50, 120] mJy.

Table 5 shows the number of potential targets for three ranges of flux densities. Of 7 targets with $\delta < -45°$ without estimates of flux density, 2 are known as weak (14–18 mJy) S-band

Table 5: The source count for the zones [$-45°$, $-90°$] and [$-30°$, $-45°$] for three ranges of flux density. Column "tot" shows the total number of known VLBI sources and column "tag" shows the number of sources with position uncertainties worse than 0.3 mas. Column shows the number of sources with uncertainties > 0.3 mas, except those observed in v561a experiment.

	[$-45°$, $-90°$]			[$-30°$, $-45°$]	
	tot	tag	new	tot	tag
no flux	10	7	7	326	326
50–120	290	289	196	232	232
120–250	305	286	123	236	227
250–3000	236	145	127	156	70

Table 6: Formal uncertainties of 0521-365 and 2149-306 positions observed at Ht-Ke-Yg-Hb-Ww network in 5–6 scans scaled to have the average SNR=15.

Network	σ_α	σ_δ
	mas	mas
Full network	0.29	0.45
Only baselines with Ht	0.33	1.00
Without baselines with Ht	0.80	0.53

sources, others, observed with IVS program, are probably brighter 200 mJy. The majority of sources without known flux density with $\delta \in [-30°, -45°]$ are from the VCS9 program. Their flux density will be determined by the end of 2017. Only a few of them will be suitable for the SOAP program. We should also keep in mind that the source count was derived on the basis the total flux density. For resolved the correlated flux density at long baselines, f.e. between South Africa and Australia/New Zealand may be less and some sources will not be detected.

4 Evaluation of the amount of resources

In order to evaluate necessary number of scans per sources, experiment aua018 (20170315_a) at network Ht-Ke-Yg-Hb-Ww was analyzed. Among others, two sources, 0521-365 and 2149-306 were observed in 4–6 scans and had SNR 15–40. Formal uncertainties of 0521-365 and 2149-306 that were scaled to correspond a case when the average SNR=15 are shown in Table 6. Analysis of this table shows that 5–6 scans per source is still not sufficient to reach the target accuracy 0.3 mas. Besides, 5–6 scans per sources is barely enough to get a good image.

A trial schedule with target sources listed in Table 5 was generated. Each target source was scheduled in 6, 8, 10 scans either 4 minutes or 6 minutes long. A block of 4 strong calibrator sources was inserted every 1.25 hour in such a way that each antenna observes two sources at elevations in a range of [7°, 30°] and two sources are observed in a range of [50°, 85°]. Observations of these sources will be used for improving estimates of residual atmospheric path delay, for tying the new catalogue with the past catalogues, and for bandpass calibration. The statistics of trial schedules is presented in Table 7.

Table 7: The number of sources observed in a 24-hr sessions at Hh-Ke-Yg-Ho-Wa-Ww the network as a function of the number of scans per source. The second column shows the number of sources if integration time is 4 minutes, the third column shows the number of sources if integration time is 6 minutes.

# sca	# sou	# sou
6	30	22
8	25	16
10	20	14

5 Proposed observations

The SOAP observing program will have two phases SOAP-1, SOAP-2, and an extension phase SOAP-3. **The goal of this program is 1) to improve position accuracy of 400 sources at declinations $< -30°$ by factor of 5 down to 0.3 mas level; 2) generate images of these sources at 2.3 and 8.6 GHz; and 3) determine their jet directions**. Considering possible losses at a level of 10%, the program will require approximately 47 twenty-four hour experiments at Hh-Ke-Yg-Ho-Ww to complete. The first program SOAP-1 targets 180 sources brighter 250 mJy and requires 12 twenty-four hour experiments to complete.

- Exploratory phase SOAP-E1. Includes all sources brighter 250 mJy at declinations $< -45°$, except 38 objects observed in v561a experiment. The number of target sources: 219. Each source is observed in two scans of 4 minutes long. **Two twenty-four hour** experiments are required. The objectives of this campaign are 1) to determine the correlated flux density at the medium length baselines (Au-Au: 1000–3000 km and long baselines, Hh-Au: 8000–10000 km); 2) improve source position **by a factor of 2** to 0.8 mas level. Observing with two scans reduces of false negative when a wrong decision about source suitability may be made due to an unnoticed failure in observations. The outcome of this phase will be the source list for SOAP-A1 phase.

- Astrometry phase SOAP-A1. Includes all the sources brighter 250 mJy at declinations $< -45°$ that were detected in SOAP-E1, even those that were observed before with IVS and have position error better 0.3 mas but still do not have images. The total number of target sources will be known after analysis of SOAP-E1 observations and is expected to be close to ~ 200. Each source on average is observed in eight to ten scans of 5 minutes long. The trial SOAP-A1-01 schedule had 16 sources with 8–10 scans per source. The scan length is reduced to 2 minutes for strong sources and extended to 8 minutes for weak sources. Considering data losses at a rate of 15%, **fifteen 24-hour experiments are required**. The objectives of this campaign are 1) improve source position **by a factor of 5 down to 0.3 mas level**; 2) generate images at X and S-band; 3) determine jet direction; 4) evaluate kiloparsec scale flux density simultaneously with parsec-scale images, which allows us to determine the source compactness. The images will be derived from 80 observations per source, which is approximately equivalent to 2 scans at the VLBA. We expect jet directions will be determined for 50–70% sources. Including SOAP-E1 observations, the source position will be derived from 10–12 scans, 100–120 observations.

- Exploratory phase SOAP-E2. Includes all sources in a range [120, 250] mJy at declinations $< -45°$, except those observed in v561a experiment. The number of target sources: 123. Each source is observed in two scans of 8 minutes long. **Two 24-hour hour** experiments are required. The objectives of this campaign are 1) to determine the correlated flux density at the medium length baselines; 2) improve source position by a factor of 2 to 0.8 mas level. The outcome of this phase will be the source list for SOAP-A2 phase.

- Astrometry phase SOAP-A2. Includes all sources in a range [120, 250] mJy at declinations $< -45°$ that were detected in SOAP-E2. The number of sources is expected in a range of 200–250. Each source is observed in ten scans of 10 minutes long. **Twenty eight 24 hour experiments are required**. The objectives of this campaign are 1) to improve source position; 2) to generate images at X and S-band; 3) to determine jet direction; 4) evaluate kiloparsec scale flux density simultaneously with parsec-scale images, which allows us to determine the source compactness. The source images will be derived from 40–100 observations. We expect jet directions will be determined for 50% sources. Including SOAP-E2 observations, the source position will be derived from 12 scans, 40-100 observations.

Each experiment that runs at 1 Gbps will collect around 7.5–8.5 Tb.

Both Ht and Hh are strongly desirable since scheduling constraints reduces the number of observations Hh can participate to 50–55% level, and to 90–95% for Ht. Observations at 200 m long baselines Hh/Ht and Ww/Wa will be used for deriving kiloparsec images and estimation of kiloparsec scale flux densities. This will gives us an estimate of compactness. Station Wa is a factor of 4 more sensitive than Ww, so it will improve imaging and will be able to detect sources that Ww will not be able to detect, for instance at a very long baseline Hh/Ww.

6 Other VLBI Southern Astrometry VLBI programs

The ATNF has accepted v561 program for absolute astrometry at Pa-Hh-Ke-Yg-Ho-At-Cd-Td-Wa network. In 2017, June 16–18, a 48 hour experiment for observing 226 sources in three scans ran. Of them, 1 was not detected in neither bands, and 6 others had less than 3 detections at S-band. Median formal uncertainties in v561a: 0.6 mas. This is an improvement of a factor of 3 with respect to the parent LCS catalogue, but still not sufficient to reach the goal. It is not clear when and whether the second v561 experiment will run. There are 39 target sources in v561a with flux densities > 250 mJy. Of them, 31 were detected at all Au-Au baselines at both X ad S bands and 8 were not.

There are target 459 sources in the declination zone $[-45°, -30°]$ with flux densities in a range 50–250 mJy and 70 target sources brighter 250 mJy. It is suggested to include them in AOV observing sessions at the core network Sh(T6),Km,Ur,Kb,Ho,Ww,Yg,Ke. We suggest to target the sources with flux densities in 50–250 mJy in observing sessions with T6 and Km and to target the sources with flux densities brighter 250 mJy with observing sessions with T6 and Km stations.

A number of trial schedules were generated. Analysis of trial schedules showed that 30 sources at declinations in a range $[-45°, -30°]$ can be included in AOV experiments and observed in three scans of 4 minutes long. Due to the network geometry, the AOV network cannot observe sources in a declination range $[-45°, -30°]$ as primary targets and fill the schedules with only these sources: it can observe them only in addition to other program sources. It will require 6 experiments to observe all the target sources with flux density brighter 250 mJy in 6 scans and approximately 16 observing sessions to observe the sources with flux densities in a range of [120, 250] mJy in 6 scans each.

The VLBA program that targets *Gaia*/VLBI counterparts brighter 150 mJy at declinations $> -40°$ was suggested to the Long Baseline Observatory. The proposal is under review. If the program will be accepted, the number of remaining target sources at declinations $[-45°, -30°]$ will be reduced by 35–40%.

7 Ad hoc experiments with Td

One of Tidbinbilla stations DSS34, DSS35, or DSS36 may be available for short VLBI sessions 4–8 hours long. These sessions are suitable for the exploratory SOAP-E3 campaign targeting sources with flux densities in a range of [50, 120] mJy. If each target sources is observed in two scans of 6 minutes each, 18 sources can be observed in a 6 hour long sessions. In total, 12 six-hour sessions are needed to observe 196 target sources in the declination zone $[-90°, -45°]$ and 14 sessions are needed to observe 232 sources in the declination zone $[-45°, -30°]$. **Position accuracy improvement of a factor of 2 from 1.5 to 0.8 mas level is expected from SOAP-E3 campaign**.

8 Expected science

Approximately 1/2 target sources have a counterpart with *Gaia*. These sources are the priority targets. The projection of the *Gaia*/VLBI offset to jet direction, the $\mathcal{O}_\mathrm{j}$ observable, provides important information about optical structure of active galactic nuclei at milliarcsecond level, not accessible by any other technique. The $\mathcal{O}_\mathrm{j}$ observables can be used in two ways: for a statistical study of the population and for study of individual sources that exhibit strong optic variability.

The following dependencies can be studied.

- $\mathcal{O}_\mathrm{j}$ versus radio core dominance defined as the ratio of the core radio flux density to the flux density integrated over the VLBI image. The sources with large positive $\mathcal{O}_\mathrm{j}$ should have a larger share of synchrotron jet emission. We expect low radio core dominance, i.e., larger contribution of jet emission, will correlate with large positive $\mathcal{O}_\mathrm{j}$. This will be an important result for modeling jet SEDs and confirming our original interpretation of the discovered effect.
- $\mathcal{O}_\mathrm{j}$ versus Doppler factors, δ (see e.g. Hovatta et al. 2009). The jet is expected to be much brighter for larger Doppler factors. For such sources the optical jet emission should win against the contribution of the accretion disk which emission does not depend on δ and therefore, high-δ jets should show larger positive $\mathcal{O}_\mathrm{j}$. Much more Doppler factors estimates will become available soon from an ongoing analysis of large monitoring programs, such as the OVRO program (Richards et al. 2011). This will be also important for jet SED modeling and confirming our interpretation.
- $\mathcal{O}_\mathrm{j}$ against optical color. The *Gaia* DR2 scheduled for 2018 Q2 will provide mean flux estimates at G and B filters. PanSTARRS provides mean fluxes at G, R, I, Z, and Y filters. We will search in literature UV fluxes as well. Sources with inverted optical spectrum are expected to have larger accretion disk contribution and show smaller positive or even negative $\mathcal{O}_\mathrm{j}$ since the accretion disk peaks in the UV-range (the so-called Big Blue Bump, see, e.g., Elvis et al. 1994).
- $\mathcal{O}_\mathrm{j}$ against object type: radio galaxies, BL Lac objects, quasars. The unified scheme of active galactic nuclei (AGNs) (e.g., Urry & Padovani 1995) explains the difference between the optical classes of AGNs by the difference in observing angle of their jets. We will independently check the unified scheme by looking for the expected correlation: a larger observing angle should result in a larger $\mathcal{O}_\mathrm{j}$ after the disk contribution is taken into account.
- $\mathcal{O}_\mathrm{j}$ against distance for AGNs with known redshift as closer targets are expected to show a stronger effect due the higher linear resolution of the observations. A cosmological evolution of the effect would be interesting to look for but is arguably complicated due to a number of possible biases.

Joint analysis of $\mathcal{O}_\mathrm{j}$ time series and light curves will be deterred to the availability of *Gaia* position time series scheduled for DR4 in 2022. When *Gaia* position time series will become available, the combined analysis of $\mathcal{O}_\mathrm{j}$ time series and optical light curves will allow us investigate individual AGNs and try to solve the following problems:

- Determine the regions where optical flares occur: in the accretion disks, in the jet base, or in the extended jet.
- Determine the optical core-dominance, the ratio of flux in the optical core jet to the total flux for the sources with flares in the core-jet regions.
- Correlate optical core-dominance with radio core-dominance. Extend SED of the core and jet from radio to optical regions and compare with results based on ~ 20 known resoled optical jets for the sources with flares in the core-jet regions.
- Determine the ratio of emission in the core and in the accretion disks for the sources with flares in the accretion disk.

The technique for solving these problems is outlined in Petrov & Kovalev (2017b).

References

Elvis, M., Wilkes, B. J., McDowell, J. C., et al. 1994, ApJS, 95, 1.

Hovatta, T.; Valtaoja, E.; Tornikoski, M.; Lähteenmäki, A., A&A, 2009, 494, 527.

Lindegren, L., et al., A&A, 2016, 595, 4L.

Kovalev, Y.Y. Petrov, L., Plavin, A., 2017, A&A, 598, L1.

Petrov L., C., Phillips, A. Bertarini, T. Murphy, E. M. Sadler, 2011, MNRAS, 414(3), 2528–2539.

Petrov, L., & Kovalev, Y.Y. 2017a, MNRAS, 467, L71.

Petrov, L., & Kovalev, Y. Y. 2017b, MNRAS, 471, 3775–3787.

Richards, J., et al., 2011, ApJS, 194, 29

Urry, C. M., & Padovani, P. 1995, PASP, 107, 803.